


Analysis and control of energy transfer processes and luminescence across the visible spectrum in PFO:P3OT blends

Wesley Renzi¹ · Flavio Franchello¹  · Neusmar J. A. Cordeiro¹ · Vitor B. Pelegati² · Carlos L. César² · Edson Laureto¹ · José L. Duarte¹

Received: 22 May 2017 / Accepted: 14 August 2017 / Published online: 22 August 2017
© Springer Science+Business Media, LLC 2017

Abstract A systematic study of luminescence from blends made of poly (9, 9-dioctylfluorene-2, 7-diyl) (PFO) and poly (3-octylthiophene-2, 5-diyl) (P3OT), and its photophysics was carried out. Acceptor concentration influence and sample preparation conditions was analyzed, particularly regarding the solvent, in order to control emission through the entire visible spectrum, and to understand the physical processes involved. An additional emission band observed in PFO:P3OT films with low concentration of P3OT was studied through confocal luminescence microscopy and was attributed to a decrease of energy transfer between P3OT molecules leading to an emission through chains with smaller conjugation length. The extra emission was also separated from the others by Time Resolved Emission Spectroscopy due to the fact that its lifetime is longer than those of the other emissions. Balance control of the emission through PFO (blue), low conjugation chains of P3OT (green) and P3OT aggregates (red) was possible changing the solvent and the way to prepare samples, that causes a greater or lesser amount of β phase in PFO. The study of the energy processes involved was also performed.

1 Introduction

Organic semiconductors are of great technological interest especially for optoelectronic applications such as organic light emitting devices (OLEDs) [1–4], organic photovoltaics (OPVs) [5–8] and organic field-effect transistors (OFETs) [9, 10]. Their main advantages are the easy processing conditions, favorable mechanical properties (flexibility) and especially the possibility of tuning their optical and electronic properties. The manufacture of organic devices active region is usually carried out by depositing a layer of organic material on another, but when using solution-processed deposition techniques (such as spincoating) it is necessary for the solvents used to deposit subsequent layers to be orthogonal. An alternative method is the use of polymer blends as the active layer of organic devices. Polymeric blends are of great importance, both for applications in organic devices (OLEDs and OPVs mainly) and for the study and development of materials with new properties.

A very promising application of organic emitters is the fabrication of white organic light emitting diodes [11–13] (WOLEDs) which emit light throughout the entire visible spectral range. WOLEDs are generally prepared by thermal evaporation of small molecules layers or by solution processable polymers. The manufacture of WOLEDs using blends of two or more solution processable polymers has the advantage of being simple to prepare and allowing the production in large areas, which is particularly attractive for application in backlight for display panels, and mainly for solid-state lighting, allowing the lighting in large areas. In order to achieve white emission, it is necessary for the device active layer to be composed of materials that emit the three primary color components (RGB), which are usually obtained by a donor blue emitting material (B), a green (G) and a red (R) acceptor emitting materials. They can be mixed

Electronic supplementary material The online version of this article (doi:10.1007/s10854-017-7714-8) contains supplementary material, which is available to authorized users.

✉ Flavio Franchello
f.franchello@gmail.com

¹ Department of Physics, Universidade Estadual de Londrina, Londrina 86057-970, Brazil

² Institute of Physics Gleb Wataghin, Universidade Estadual de Campinas, Campinas 13083-859, Brazil

in a solution, thereby providing a blend emitting throughout the entire visible range, which can be deposited on a suitable substrate.

Studies on polymer blends for WOLEDs applications [14, 15] have been challenged to find a better ratio of materials to balance the emitted radiation. By reducing the amount of acceptor molecules, it is possible to saturate their emission and therefore the energy transfer, allowing emission by donor molecules. Generally, it is very difficult to establish a good relation between emitting materials (R, G, B) to obtain a good white emission [16] (CIE $x=y=0,33$). Therefore, the study of the optical properties of polymers and their blends have great importance for the development of new devices.

A class of conjugated polymers that has been widely used in WOLEDs is polyfluorenes. A prototypical fluorene-based homopolymer is poly(9, 9-dioctylfluorene) (PFO), which is used due to its pure blue emission, high photoluminescence quantum efficiency, and high hole mobility [17]. The PFO molecule has different solid phases, from which the glassy phase [18] is more likely to form when samples are spin coated. However, a more ordered structural conformation, known as β phase, can also be formed, where the rotational angle between the monomer units is 180° [17, 19]. The spectroscopic properties of both phases are clearly different. Regarding absorption, the glassy film shows a broad band with a maximum around 3.23 eV (384 nm) while the β phase shows a narrow, well-resolved absorption peak at 2.84 eV (437 nm) [18]. According to Ariu et al. [17], emission spectrum at room temperature (RT) of a glassy film has emission peaks at 423, 447, 476 and 502 nm, while the peaks in the RT β -phase PL spectra are at 440, 468, 500 and 533 nm, and the peak at 440 nm is assigned to the $S_1 \rightarrow S_0$ 0–0 transition [18, 20]. As the β -phase chains have a smaller energy gap, it is very common for the emission related to the glassy phase not to be observed due to the excitation energy transfer from the glassy to the β -phase.

Poly(3-alkylthiophene) (P3AT) are polymers whose monomer, the 3-alkylthiophene (3AT) is constituted by a thiophene ring, a sulphur heterocycle, with an alkyl side group attached to the position 3 of the ring. The alkyl groups have the formula C_nH_{2n+1} and are responsible for solubility. P3ATs are soluble in many organic solvents and have interesting properties such as electrochromism [21], thermochromism [22], solvatochromism [22, 23] and luminescence [24–26]. The optical properties changes of P3ATs are induced through twisting of the polymer backbone, which disrupts the conjugation, once the conjugation relies upon overlap of the π orbitals of the aromatic rings. The absorption and luminescence bands in the visible range red shift as the conjugation length increases. Xu and Holdcroft [27] showed that the emission maxima of the poly(3-hexylthiophene) (P3HT) occur at increasing energy (lower wavelengths) with increasing head-to-head (HH)

dyad content due to steric interactions between adjacent 3-alkylthiophenes, which twist the conformation of these rings and, consequently, break the conjugation. They also showed that P3HT thin films have higher quantum yields for the less planar configurations, which contain higher fractions of HH dyads. In this case, the classical concentration quenching effects are reduced, due to non-emissive excimer complexes. Taking into account the properties of PFO and P3ATs discussed above, and the fact that the PFO emission and the poly(3-octylthiophene) (P3OT) absorption spectra overlap, the blend PFO:P3OT is a very interesting system to be investigated in order to have a control of energy transfer mechanisms and emission in a very broad spectral region. That is very promising for WOLEDs and other applications, for example, the change of the physical properties of this family of polymer blends on different substrate surfaces [28].

In this work, a systematic study of the emission from a PFO:P3OT polymeric blend was carried out. Acceptor concentration and sample preparation conditions, particularly the solvent, were analyzed aiming at understanding the influence of these conditions on optoelectronic properties. These results can be used to control the emission across the whole visible spectrum, as well as to understand the physical processes involved. Initially, absorption and emission spectra were obtained from PFO and P3OT films and a PFO:P3OT film with a low concentration of the dopant (P3OT). In order to understand the nature of an intermediate emission, which appears between PFO and P3OT emissions for low dopant concentrations, emission from diluted solutions of P3OT were measured, as well as confocal microscopy and micro-PL from PFO:P3OT blend films. Time decay measurements and TRES were also performed, thus enabling the separation of this intermediate emission (longer lifetime) from the other contributions. As the PFO:P3OT emission spectrum in toluene (at lower concentrations) shows emission in the whole visible spectrum, a systematic study of the solvent influence on the emission, as well of the energy transfer and the dynamics of the physical process involved was performed.

This paper is organized as follows: samples and experimental setups details are described in Sect. 2. In Sect. 3, results and discussions are presented, and in Sect. 4, conclusions can be seen.

2 Samples preparation and experimental methods

2.1 Samples preparation

Polymers used were regioregular P3OT [poly(3-octylthiophene-2,5-diyl)], ($M_w = 20.000\text{--}70.000$), from American Dye Source, and PFO [poly(9,9-dioctylfluorenyl-2,7-diyl)] ($M_w \geq 20.000$) from Aldrich, whose monomers are shown in Fig. 1a and b, respectively.

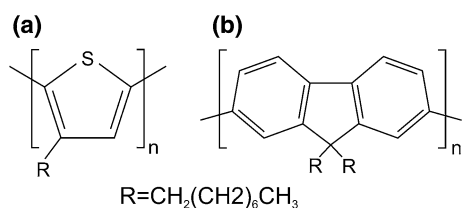


Fig. 1 Monomer molecular structure of **a** P3OT and **b** PFO polymers

The polymer solutions were deposited by spin coating (1000 rpm for 60 s) on glass slides, which were washed in an ultrasonic cleaner for 30 min (15 min in acetone + 15 min in isopropyl alcohol). The samples were dried for 2 h at room temperature ambient conditions. PFO (in chloroform) samples were dried in two different ways: 2 h in room condition or 15 min in vacuum condition. All samples were deposited using 8 mg/mL solution concentration diluted in toluene, chloroform (CHCl_3) or Dichlorobenzene (DCB). Homopolymer films (P3OT and PFO) were deposited, as well as PFO:P3OT blends with the following wt% of P3OT: 2.5, 5, 10 and 20%.

2.2 Experimental methods

The absorption spectra were measured by a UV–Vis spectrometer (Shimadzu UV-2600). The photoluminescence spectra (PL) were obtained using as excitation source a diode laser at 375 nm, a diode laser at 405 and the 488 nm line of an Ar^+ laser. Emissions were detected by an Ocean Optics USB2000+ Spectrometer. Photoexcitation measurements were performed using a 300 W Xenon lamp and two monochromators: one as an excitation source (Newport—Cornerstone) and the other for detection (0.5 m focal length, Jarrel-Ash). The photoexcitation signal was detected by a GaAs tube photomultiplier (Hamamatsu R636-10). Photoluminescence decay time and TRES measurements were performed using a Fluo Time 200, from PicoQuant, that uses the time-correlated single photon counting (TCSPC) technique and is equipped with a MCP detector, and 375 nm diode pulsed laser (10 MHz). The TRES measurements were performed automatically with a 5 nm step in the detection wavelength, from 400 to 520 nm for the PFO and 400 to 700 nm for the PFO:P3OT (5% blend). The morphological characterization of the blends was obtained by confocal fluorescence microscopy using a Zeiss Upright LSM780-NLO equipment. Confocal fluorescence images were recorded with excitation wavelength at 405 and 488 nm, and the emission was collected from 400 to 700 nm.

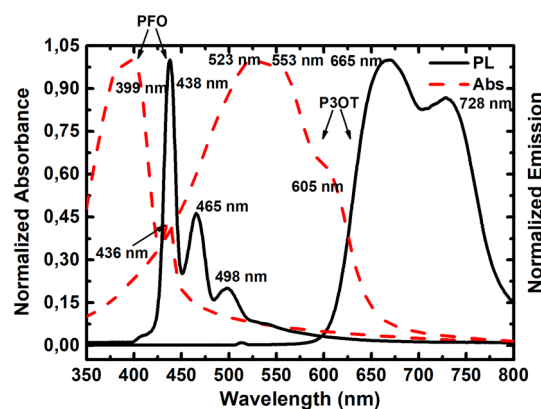


Fig. 2 Normalized absorbance and photoluminescence of PFO and P3OT films (toluene) with excitation at 375 nm (PFO) and 514 nm (P3OT)

3 Results and discussion

Initially, absorption and emission of the blend components: PFO and P3OT, and blend PFO:P3OT with different concentrations of P3OT, using toluene as solvent, were measured.

Figure 2 shows the absorption and emission spectra from PFO and P3OT films prepared with toluene. The wavelengths of the absorption and emission peaks are highlighted.

The spectra in Fig. 2 were normalized in order to make a clear comparison between them. The PFO absorption band is broad and has a maximum at $\lambda_{\text{abs}} = 399$ nm with a low intensity peak at $\lambda_{\text{abs}} = 436$ nm, showing that during the film formation some chains are arranged in the β -conformation, a more planar orientation of the backbone [17–20]. The P3OT shows a large absorption band with maxima at 523 and 553 nm, and a shoulder at 605 nm. As analyzing PFO and P3OT individual polymers photoluminescence (PL) spectra (solid lines in Fig. 2), the observed transitions were identified as follows: The PFO film sample has three emission peaks related to the 0–0, 0–1 and 0–2 (purely electronic first and second vibronic bands, respectively) transitions [17, 18, 20], at 438, 465 and 498 nm, respectively. However, P3OT presents two emission peaks of aggregates [29, 30], centered at 665 (0–0) and 728 nm (0–1), respectively.

The overlap between the PFO PL spectrum and the P3OT absorbance spectrum can be observed in Fig. 2, indicating the possibility of energy transfer from PFO (donor) to P3OT (acceptor) when the excitation wavelength is within the PFO absorption range. Figure 3a shows the absorbance spectra of the blend samples (5, 10 and 20% of P3OT), where an increase in absorption at 450–650 nm spectral region (absorption of P3OT) is observed with increasing P3OT concentration in the blend.

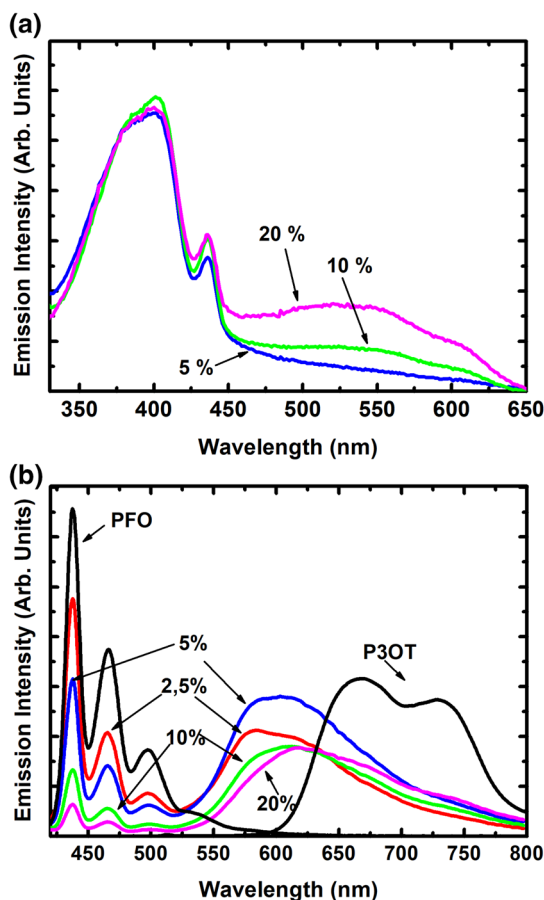


Fig. 3 a Blend samples absorbance of PFO:P3OT in different relative concentrations of P3OT; b photoluminescence (excitation at 375 nm) spectra of individual PFO, blend samples of PFO:P3OT, and individual (excitation at 514 nm) P3OT

Figure 3b presents the PL spectra of PFO and blend samples, with excitation at 375 nm, and PL spectrum of P3OT with excitation at 514 nm, once the emission of P3OT, when excited at 375 nm, is in the limit of detection. Regarding the photoluminescence spectra of the blends, the highest and the lowest energy transitions are related to PFO and P3OT, respectively, as expected. However, in addition to those emissions, a broad and intense band emission with intermediate energy is also observed, in such a way that the resulting emission covers the whole visible spectral region. As the concentration of P3OT decreases, the maximum of this intermediate emission shifts to lower wavelengths (higher energies), and its intensity increases for concentrations as low as 5% and decreases for 2.5% concentration.

In order to separate these contributions, PFO:P3OT blends spectra were fitted by Gaussian curves, only to roughly find the peak positions. The fit for the 5% blend is shown in Fig. 4 (more information is given in Supplementary material, Figs. SI.1–4 and Tables SI. I–IV). Through the Gaussian fit of the blend spectrum, it is possible to relate

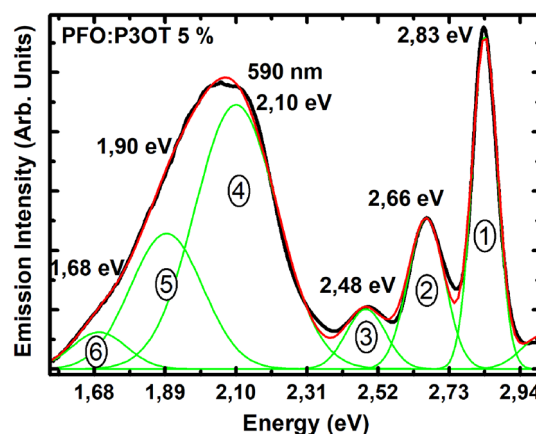


Fig. 4 Gaussian fit of the PFO:P3OT (5%) PL spectrum

peaks 1, 2 and 3 to the PFO transitions, and peaks 5 and 6 to the P3OT transitions, according to the PL spectra of polymer samples (PFO or P3OT), also shown in Fig. 2. In addition to these transitions, there is peak 4 of intermediate energy, which is not observed in the polymers PL spectra of Fig. 2. Moreover, a red shift of the intermediate peak is observed when the P3OT relative concentration in the blend decreases, as seen in Table 1.

Both the intermediate emission and the one from P3OT are due mainly to energy transfer from PFO to these emission centers, since the P3OT absorption at 375 nm is minimum. In order to confirm this hypothesis, photoluminescence measurements were performed with selective excitation at 375, 488 and 514 nm (Fig. 5a), as well as photoexcitation measurements (Fig. 5b).

Figure 5a illustrates that when the PFO:P3OT (5%) blend is excited in the P3OT absorption range (488 and 514 nm), the emission in the 530–700 nm range is very small compared with that observed when the excitation is performed in the PFO absorption region (excitation at 375 nm). This result means that the main source of emission above 530 nm is energy transfer from the PFO. Similar results were obtained when photoexcitation spectra were analyzed (Fig. 5b). The

Table 1 Intermediary peak position for different relative concentrations of P3OT in PFO:P3OT blends

P3OT relative concentration (%)	Intermediary peak	
	Energy (eV)	Wave-length (nm)
2.5	2.16	574
5	2.10	590
10	2.09	596
20	2.03	610

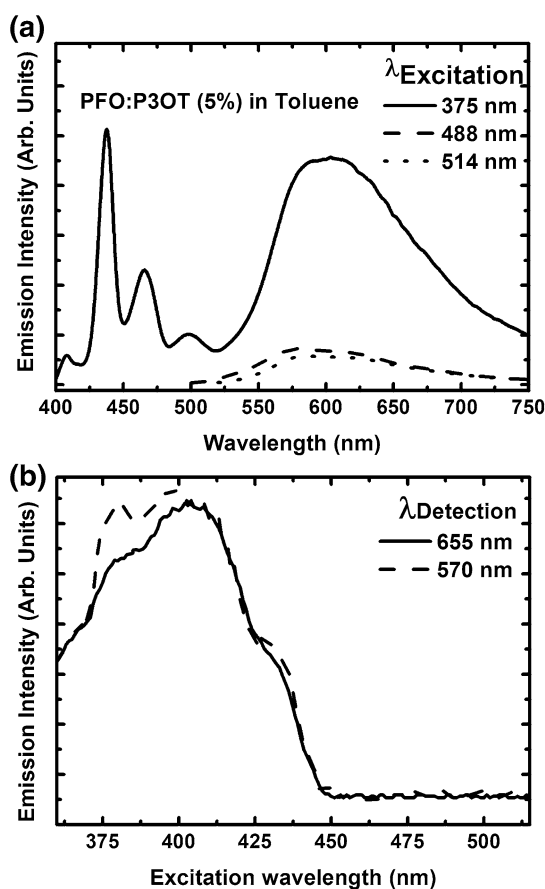


Fig. 5 **a** Selective photoluminescence spectra with excitation at 375, 488 and 514 nm; **b** photoexcitation spectra with detection at 570 and 655 nm

contribution to the intermediate peak emission (detection at 570 nm) and to the peak at 655 nm have very similar shape to the PFO absorption spectrum, proving that the results are related almost entirely to energy transfer between the polymers. This intermediate emission was also observed by F. Franchello [Ph.D. Thesis, Physics Department, Universidade Estadual de Londrina] and Santos [31] in the PFO:P3HT blends, and in Santos' work this emission was attributed to the emission of isolated P3HT chains due to the dispersion in the PFO matrix, based on comparison with the emission of low concentration solutions of P3HT.

To check the possibility that the emission band around 570 nm is due to isolated P3OT molecules emission, two tests were made: (a) emission spectra from the solutions with different concentrations of P3OT were obtained, and (b) Confocal Luminescence Microscopy of the blend films.

The photoluminescence spectra from the P3OT solutions dissolved in toluene are shown in Fig. 6.

Figure 6 shows that, at the concentration of 32 mg/mL, at higher wavelengths the emission spectrum of the solution is similar to the P3OT films spectrum, where the emission

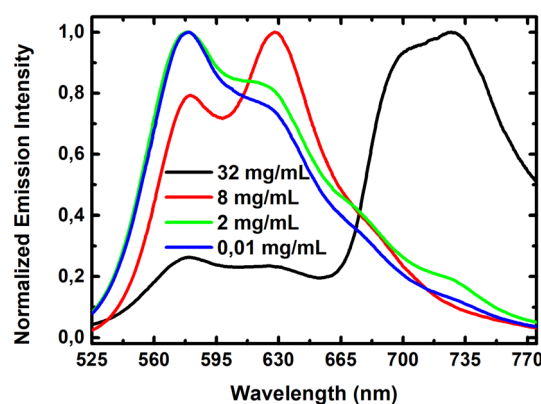


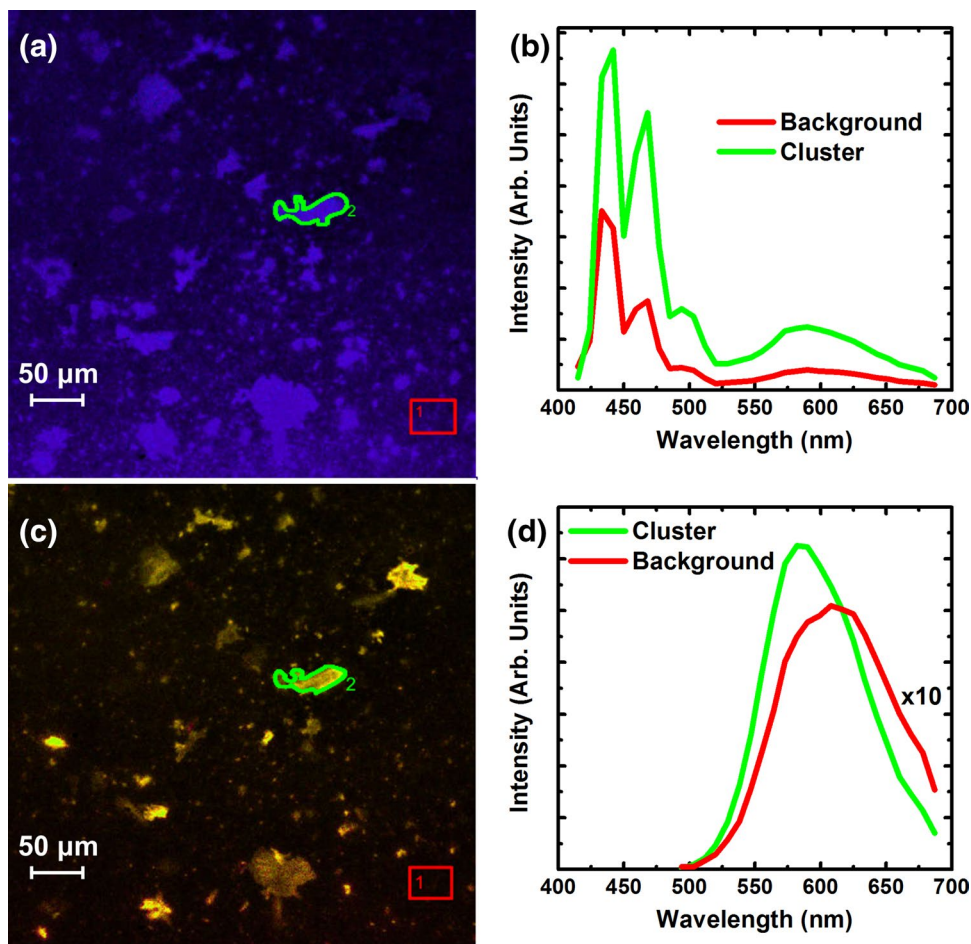
Fig. 6 Photoluminescence spectra of P3OT toluene solutions with different concentrations

is mainly due to aggregates of P3OT. However, even at this high concentration, a peak at 575 nm appears. As concentration decreases, this lower energy peak has a relative increase compared to the others, and for 2 mg/mL concentration, it is already dominant. This is a strong evidence that the emission around 570 nm is due to the isolated chains, as proposed by Santos et al. [31] for the P3HT. In the case of P3OT, the peak at 575 nm begins to appear at higher concentrations than for P3HT, due to the longer side chains of the P3OT.

However, when films are analyzed, this comparison must be carefully interpreted, despite the resemblance of the solution and film emissions. While in solutions there is a constant movement of the molecules, leading to a dynamic interaction between the polymer and solvent; in film this behavior is different, resulting in a solid state morphology that can be affected by many factors, as solvent evaporation and a stronger polymer–polymer interaction. In addition, it is necessary to take in account the PFO, as a matrix in the blend film, which may interact with the dopant, changing its emission. In order to have a better understanding of the blend films emission based on its morphology, solid state samples of the PFO:P3OT were analyzed. Confocal luminescence microscopy was performed and the emission was analyzed by exciting the blend at different wavelengths, 405 and 488 nm. At 405 nm, mainly the PFO is excited, allowing analysis of the blend total emission, while at 488 nm the intention is to excite the P3OT but not the PFO.

The image presented in Fig. 7a (with excitation at 405 nm) shows formation of clusters in the blend films, seen as brighter areas. Spectra were obtained in two distinct regions: inside the cluster (region delimited by the green line) and outside it (region delimited by the red line). The spectra shown in Fig. 7b, both inside and outside the cluster region, show the emission from the PFO (in the beta phase) and a featureless broadband emission around 580 nm. It is also possible to notice that in the cluster region the emission

Fig. 7 Confocal microscopy images of the PFO:P3OT (95:05) blend, excited at **a** 405 nm and **c** 488 nm. Emission spectra of the highlighted regions (green and red) with the excitation at **b** 405 nm and **d** 488 nm. (Color figure online)



is more intense. Figure 7c shows the image obtained with the laser at 488 nm, exciting almost only the P3OT. The image of these clusters is observed, indicating that the emission of P3OT occurs also mainly through them. This is confirmed when the relative emission intensities are compared (Fig. 7d), showing that in the cluster region the emission is around 10× more intense. In addition to that, it is also observed that the emission in the clusters is blueshifted, thus being related to the more energetic component of the P3OT total emission.

The PFO chains act by separating the P3OT molecules (mainly within the clusters), reducing the energy transfer between them, a fact verified by an increase in the lifetime of the green emission of P3OT (see Table 3). As PFO in the beta phase has a lower energy gap than the PFO in the vitreous phase (phase which is mainly excited), beta-rich regions (clusters) have an important role as recombination centers for the carriers. This provides a greater probability of energy transfer to P3OT chains that are in these regions, although the beta phase also emits a lot, which can be explained by the intercalation of amorphous phase PFO in the in the PFO beta phase regions, preventing the total quenching of its emission. These results lead us to conclude that the clusters are formed

by PFO chains (mainly in the beta phase) and P3OT. The broadband emission is due to the emission of P3OT chains of different conjugation lengths, which are separated from each other by PFO chains. Moreover, this separation prevents energy from going to lower energy levels of the P3OT, explaining the blueshift of their emission.

Confocal microscopy measurements with excitation at 488 nm were also performed on blends of different concentrations of P3OT (2.5, 5, 10 and 20%), and they are shown in Fig. 8.

In the images shown in Fig. 8 it is possible to see the change in the emission of the region outside the clusters (background). With the increase of the P3OT concentration, the emission goes from green/yellow to red. In addition, the emission of the clusters is less evident compared to the background emission, which is explained by the increase in the amount of P3OT in the film. This increase induces the formation of P3OT aggregates [32], allowing a better interaction between P3OT chains, which leads to a higher energy transfer between them, causing the emission to occur through chains with longer conjugation (lower energy), leading to a more spatially uniform and reddish emission of P3OT.

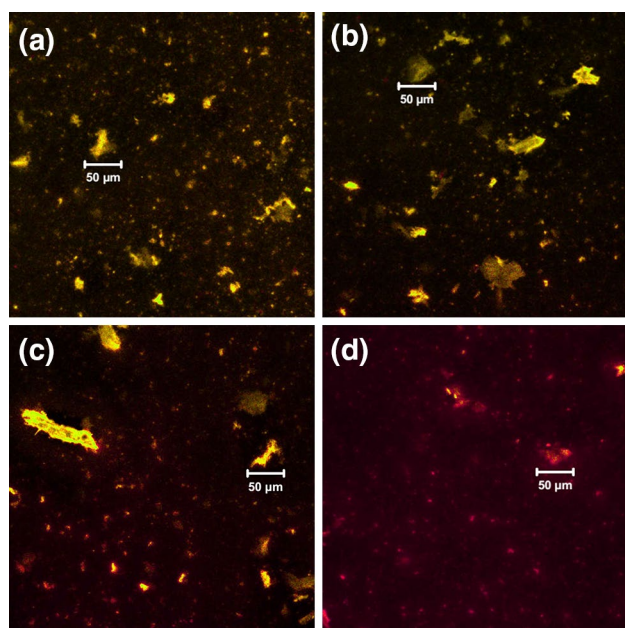


Fig. 8 Confocal microscopy images of the PFO:P3OT blend with a 2.5%, b 5%, c 10% d 20% of P3OT, excited at 488 nm

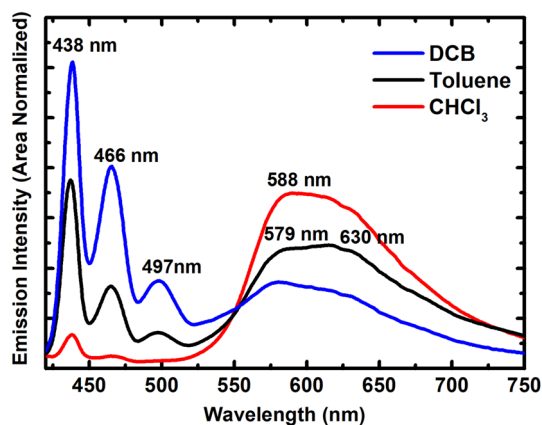


Fig. 9 Photoluminescence spectra of PFO:P3OT (5%) blend films from different solvents, with 375 nm excitation

Another interesting feature of the PFO:P3OT blend photoluminescence spectrum (Fig. 3b) is the fact that energy transfer from PFO to P3OT is partial, so that the PFO also shows an emission. This is very important for obtaining white blends. Absorption and photoluminescence behaviors of both homopolymers (PFO and P3OT) as well as of blends of PFO:P3OT (5%) using chloroform (CHCl_3), dichlorobenzene (DCB) and toluene as solvents were studied. The spectra of the PFO:P3OT (5%) blends prepared with these solvents are shown in Fig. 9.

In Fig. 9, it is noticeable that solvent change affects strongly the relative intensities of the emission peaks, i.e., directly affects energy transfer between polymers. In the

case of CHCl_3 , a very volatile solvent, even with only 5% of P3OT, the PFO emission almost entirely quenches, transferring its energy to the P3OT. When using less volatile solvents such as toluene and DCB, a lower energy transfer is observed. According to Ariu et al. [17] and other authors [33, 34], PFO can show two main conformations for their chains, known as glassy phase and crystalline phase (β phase). The formation of one or other of these phases can be influenced by subjecting the sample to certain vapors [35] or by dipping the films into solvents [36]. Known for its greater regularity, the β phase has a 180° rotation between PFO units, allowing the polymer to have longer chains, and, consequently, with lower emission energies (with the peaks at 438, 465 and 497 nm) [18, 20]. In the glassy phase, chains are less organized and have shorter conjugation (with peaks at 421, 442 and 477 nm) [17–20]. A significant feature of the β phase is the appearance of a narrow peak at around 436 nm [18] on the absorption spectrum. The formation of the β phase is favored by slower evaporation, where the PFO chains have a longer time to rearrange. The β phase is commonly observed in less volatile solvents such as toluene and DCB. In the case of more volatile solvents, such as CHCl_3 , the chain rearrangement time is short, hindering the formation of more regular structures.

To highlight the formation of different phases, four types of samples were prepared using DCB, toluene and CHCl_3 (two different samples). For samples in CHCl_3 , two types of drying were performed: in vacuum (sample A), seeking a quick evaporation of the solvent, and therefore the amorphous phase formation; drying in a saturated atmosphere (sample B), thus hindering the solvent evaporation, seeking the formation of β phase. The absorption and emission results are shown in Fig. 10.

An important point regarding the different phases existing in PFO is that, whenever β phase appears, it is accompanied by the glassy phase as well, which has higher energy (as can be seen in the absorption spectra). However, when the two phases are present, photoluminescence usually shows just the lowest energy peaks corresponding to β phase, due to energy transfer from chains of the amorphous phase to the β phase, which act as a trap [33]. Therefore, it is possible to understand that in sample A, for which a volatile solvent was used and had a very fast drying process, only glass phase was formed, thus it only shows emissions corresponding to that phase (peak 0–0 at 421 nm). However, for sample B (in CHCl_3), prepared using the same solvent, but having a slower drying, the spectrum shows a shoulder at 421 nm (glassy phase) and a main peak at 438 nm (β phase). The shoulder at 421 nm only appears because the β phase fraction is too small (as shown by the absorption spectrum) and, therefore, some of the glassy phase chains do not have how to transfer energy to the β phase and they emit by themselves. For samples prepared in toluene and DCB,

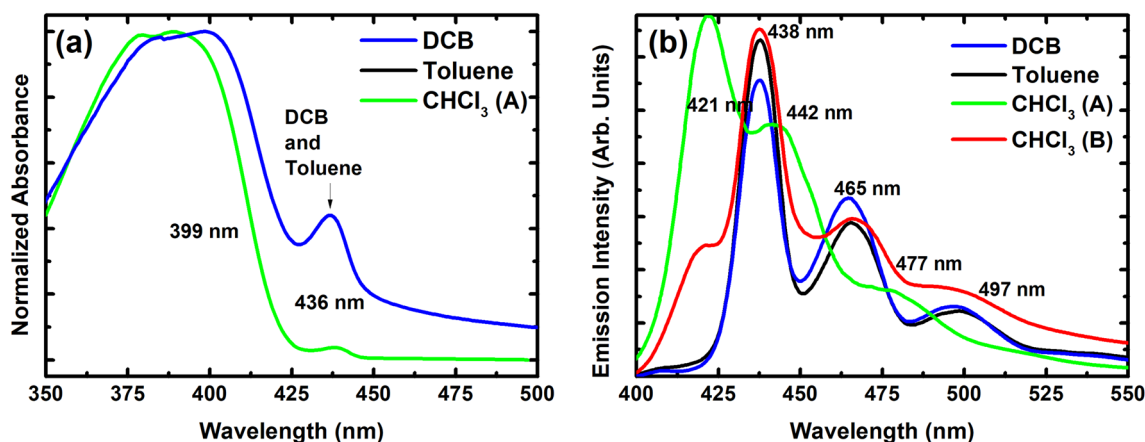


Fig. 10 Normalized absorbance (a) and photoluminescence (b) spectra of PFO films in different solvents. In absorbance, DCB and Toluene curves overlap completely, while in CHCl_3 , the drying process causes different behaviors both in absorption and in PL

wherein the drying is slower and thus the β phase formation is higher (as shown by the absorption spectrum), all energy is transferred to the β phase and, thus, only emission due to this phase appears.

According to what was discussed in the last paragraphs, Fig. 9 [PL spectra of PFO:P3OT (5%) blend films in different solvents] can be analyzed more carefully. In this figure, the spectrum of the sample prepared in CHCl_3 , which has mainly PFO in the glassy phase, shows that, when this phase is excited, energy transfer occurs mostly to P3OT and consequently, emission occurs in almost all the spectral region of green, orange and red, with a very weak emission in the blue (β phase). For samples prepared in DCB and toluene, which have a higher rate of β phase, emission in blue is large, due to this phase. However, samples prepared with toluene have a better balance between intensities observed throughout the visible spectrum. In this case, excitation of the glassy phase, which has a broad absorption band, causes energy migration between the chains of this phase, until excitation finds any of the following light emitting centers: PFO chains in the β phase, aggregates of P3OT and P3OT chains of different conjugation lengths that are separated from each other, and; so, there is emission by all those centers.

Figure 11 shows results of TRES measurements of a PFO film sample processed in chloroform, showing the temporal evolution of the emission spectra. In these spectra, one can see, immediately after the excitation, emission from both the β phase and the glassy phase. After a lapse of time less than 300 ps, almost all the energy was transferred to the β phase, while nearly no emission from the glassy phase was seen, but only a small contribution that persists for a longer time and it is attributed to isolated small regions of the glassy phase.

To complement the analysis of emission and energy transfer mechanisms, emission decay time at 438, 466

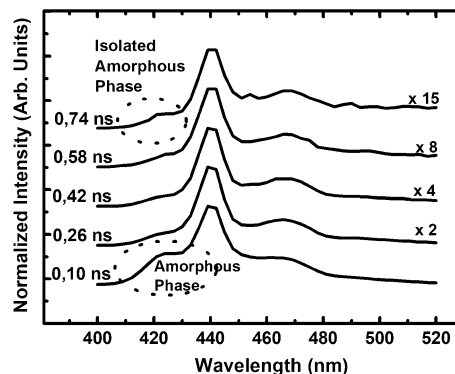


Fig. 11 Time resolved emission spectroscopy spectra of PFO film (CHCl_3)

and 497 nm (β phase) on the PFO film, as well as the emission at 650 and 730 nm in the P3OT sample and the emission at 438, 466, 497, 580 and 650 nm of the blend PFO:P3OT (5%) were measured. The decay spectra of the PFO and P3OT toluene films are shown in Fig. 12, with the decay adjustments parameters presented in Table 2. For the emission at 438 nm (β phase) obtained for PFO homopolymer film, a predominant lifetime of 210 ps (93% contribution) and a small contribution (7%) with a long lifetime, which can be associated with isolated chains of PFO in this phase, are observed.

For the PFO:P3OT (5%) blend the decay measurements are shown in Fig. 13, and the decay parameters are shown in Table 3.

From Table 3 it is possible to see that the time of the main PFO decay channel decreased to 80 ps. From this result, one can conclude that, besides having transfer from glassy phase to the β phase (PFO) and to P3OT, there is also energy transfer from the PFO β phase to the P3OT,

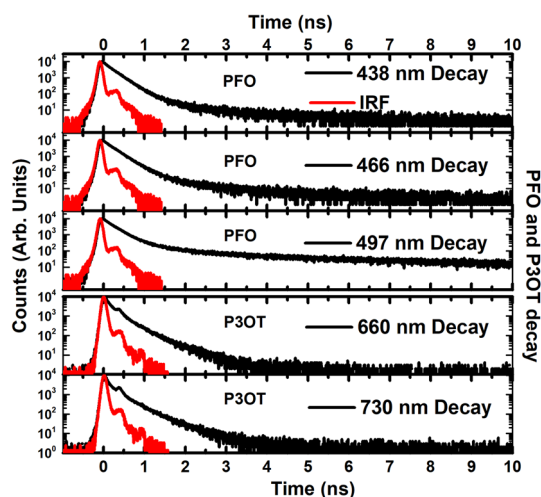


Fig. 12 Emission decays for the PFO (438, 466 and 497 nm) and P3OT (660 and 730 nm) films deposited from toluene solution

Table 2 Emission decay times for the PFO and P3OT films

Detection (nm)	τ (ns)	$\Delta\tau$ (ns)	Con-tribution (%)
PFO film (toluene)			
438 nm	0.79	0.02	7
	0.21	0.01	93
466 nm	0.91	0.03	7
	0.22	0.00	93
497 nm	3.83	0.16	15
	0.25	0.00	85
P3OT film (toluene)			
660 nm	0.55	0.01	24
	0.21	0.01	76
730 nm	0.67	0.03	18
	0.25	0.01	82

which occurs with a transfer efficiency of approximately 60%.

Decay time measurements of the PFO:P3OT (5%) films at 580 and 650 nm show two different lifetimes for each emission, a long (~5 ns), and another relatively short (~680 ns). The longer and predominant component (5.25 ns) at 580 nm, can be explained by the difficulty to occur energy transfer among the P3OT chains related to the blueshifted component of the emission, as discussed before. As this emission is broadbanded, its influence is still noticed when the emission is analyzed at 650 nm, however with a smaller contribution and slightly lower lifetime (4.63). The faster decay (~0.7 ns) is related to the P3OT well ordered aggregates. The aggregation of P3OT leads to a better energy transfer, reducing the lifetime and redshifting the emission.

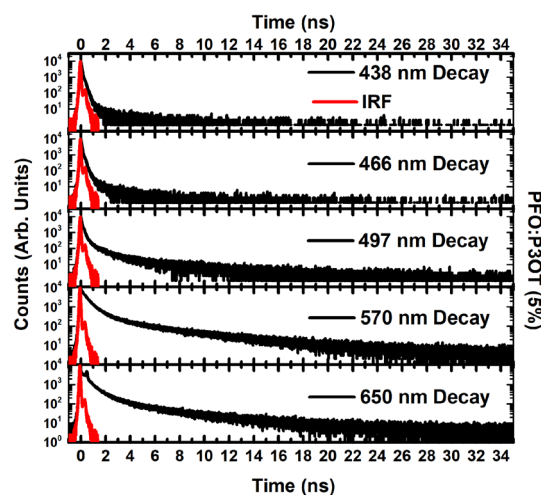


Fig. 13 Emission decays for the PFO:P3OT (5%) films cast from toluene

Table 3 Emission decay times for the PFO:P3OT (5%) blend

Detection (nm)	PFO:P3OT (5%) film (toluene)		
	τ (ns)	$\Delta\tau$ (ns)	Con-tribution (%)
438 nm	0.28	0.01	15
	0.08	0.00	85
466 nm	0.48	0.02	10
	0.09	0.00	90
497 nm	1.65	0.08	22
	0.15	0.00	78
580 nm	5.25	0.11	59
	0.69	0.02	41
650 nm	4.63	0.08	40
	0.68	0.01	60

As the decay time of the isolated chains is much longer than that of the agglomerates, TRES spectra were obtained in order to separate the spectra of these emissions at different times. The result is presented in Fig. 14.

In Fig. 14, TRES spectra are shown. They were normalized whilst maintaining the highest point at the same height and the multiplication factor needed for its normalization is not shown, but increases with the delay time up to 250 times. In this figure, it is possible to see how blend emission evolves over time. Between 0.05 and 1.25 ns it is possible to observe a decrease in the contribution of the PFO emission (around 450 nm) and between 0.85 and 1.05 ns an emission appears around 650 nm, which is due to P3OT aggregates. At 1.45 ns, it is already possible to observe the dominance of the broad band assigned to the energetically isolated chains with different conjugation lengths, around

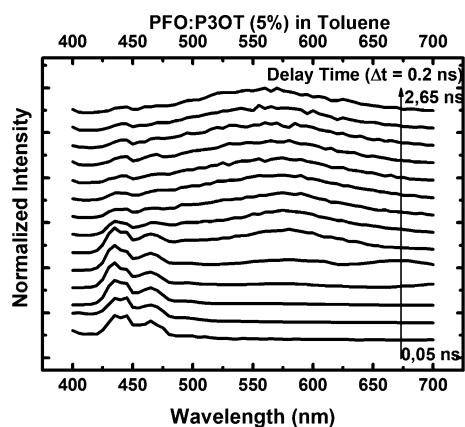


Fig. 14 TRES spectra of the PFO:P3OT (5%) blend films with 375 nm excitation

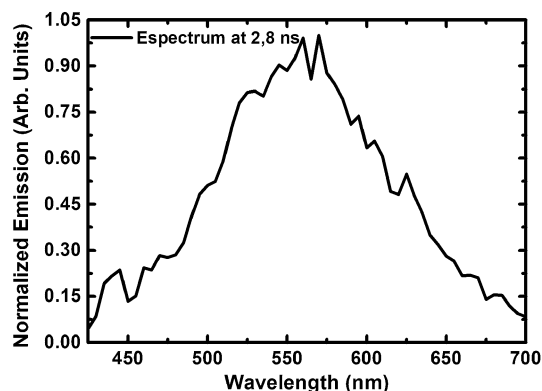


Fig. 15 Normalized TRES (2,8 ns after pulse) spectrum for PFO:P3OT (5%)

575 nm. For longer time, the maximum shifts slightly to lower wavelengths due to the contribution of isolated P3OT smaller chains.

Figure 15 illustrates the emission spectrum for the PFO:P3OT (5%) at 2.8 ns (excited at 375 nm), where a broad emission centered on about 550 nm is shown. This broad emission is characterized by a large conjugation length distribution of energetically isolated chains.

4 Conclusions

In this work, a study of energy transfer processes and emission of PFO:P3OT blends was performed, varying the acceptor concentration and the conditions of sample preparation, particularly the solvent, in order to analyze the conditions that may affect emission control across the visible spectrum.

The PFO:P3OT (5%) blend emission in toluene, in addition to PFO and P3OT emissions, showed an intense intermediate emission. Confocal luminescence microscopy

results of the blend showed that P3OT is distributed in two main ways in the film: as isolated molecules inside the beta phase PFO clusters, and as aggregates. The aggregates emission spectrum is very similar to that of a P3OT homopolymer film. The P3OT emission, inside the clusters presents a broad band, with a maximum around 580 nm, which shows clearly that the intermediate emission on the blend of PFO:P3OT (5%), is due to the emission of energetically isolated P3OT. The fact that this emission showed a broadband was attributed to different conjugation lengths of these chains. Moreover, the difficulty to occur energy transfer between P3OT molecules also allows emission through lower conjugated chains, leading to a large shift towards the green region.

From the decay time measurements, a 5 ns lifetime for the intermediate emission was observed, which is longer than the other contributions. This fact allowed, through TRES spectra, to separate, for long times, the emission of this intermediate band from the others, resulting in a broad spectrum with maximum at 565 nm. This spectrum is similar to that obtained by confocal microscopy of clusters that emit mainly in the green region, which supports the previous conclusion that the intermediate emission from the PFO:P3OT (5%) blend is due to energetically isolated small conjugated P3OT chains.

By changing the solvent and the concentration of the acceptor, it was possible to control the whole emission spectrum. When using a more volatile solvent such as chloroform, there is practically the formation of PFO only in the glassy phase, which transfers the absorbed energy almost completely to the isolated chains and to the P3OT agglomerates and thus, the emission occurs especially in the green and red region. When using a less volatile solvent such as DCB and toluene, in addition to the glassy phase (which is the majority and has broad emission spectrum), the β phase is also formed, which has lower energy and works as an energy trap and radiative emission center. In the latter case, when the glassy phase is excited, its energy migrates through the molecules of this phase and is transferred to the β phase, and to the P3OT (aggregates or isolated chains). Therefore, emission occurs across the visible spectrum.

The situation in which the energy is better distributed among the various emissions is that of PFO:P3HT (5%) blend in toluene. Although the β phase acts as an energy trap and an emission center, it transfers some of its energy to aggregates and isolated chains as well, which is evidenced by the decrease in the decay time of the PFO β phase emission in the presence of P3OT. Therefore, emission is well distributed among different colors.

In this way, this study allowed us to understand energy transfer processes between the main emission centers and the dynamics of these processes, as well as to control the

resulting emission across the visible spectral range, which, in its turn, is of great interest for making white blends.

Acknowledgements This work was supported by Brazilian agencies such as: Coordenação de Aperfeiçoamento de Pessoal de Nível Superior (CAPES), Conselho Nacional de Desenvolvimento Científico e Tecnológico (CNPq), Fundação Araucária de Apoio ao Desenvolvimento Científico e Tecnológico do Paraná (Fundação Araucária), and Instituto Nacional de Ciência e Tecnologia em Eletrônica Orgânica (INEO). The authors gratefully acknowledge Dr. Teresa D. Z. Atvars and Dr. Fernando J. Quides for their helpful discussions concerning this work, as well as ESPEC Laboratory-Central Multiusuário-PROPPG-UEL.

References

- G. Jin, L. Xia, Z. Liu, H. Lin, J. Ling, H. Wu, L. Hou, Y. Mo, J. Mater. Chem. C **4**, 905 (2016)
- D. Das, P. Gopikrishna, A. Singh, A. Dey, P.K. Iyer, Phys. Chem. Chem. Phys. **18**, 7389 (2016)
- B. Gautier, X. Wu, F. Altal, S. Chen, J. Gao, Org. Electron. Phys. Mater. Appl. **28**, 47 (2016)
- N. Vilbrandt, A. Gassmann, H. Von Seggern, M. Rehahn, Macromolecules **49**, 1674 (2016)
- H. Liu, L. Hu, F. Wu, L. Chen, Y. Chen, ACS Appl. Mater. Interfaces **8**, 9821 (2016)
- H. Heo, H. Kim, D. Lee, S. Jang, L. Ban, B. Lim, J. Lee, Y. Lee, Macromolecules **49**, 3328 (2016)
- J.B. Park, J.-H. Kim, D.-H. Hwang, Polym. Bull. **73**, 2393 (2016)
- Y. Wang, Q. Zhang, F. Liu, X. Wan, B. Kan, H. Feng, X. Yang, T.P. Russell, Y. Chen, Org. Electron. Phys. Mater. Appl. **28**, 263 (2016)
- M. Da Silva Ozorio, G.L. Nogueira, R.M. Morais, C. Da Silva Martin, C.J.L. Constantino, N. Alves, Thin Solid Films **608**, 97 (2016)
- S. Han, X. Zhuang, W. Shi, X. Yang, L. Li, J. Yu, Sens. Actuators B **225**, 10 (2016)
- Y. Zhao, Z. Lin, Z. Zhou, H. Yao, W. Lv, H. Zhen, Q. Ling, Org. Electron. Phys. Mater. Appl. **31**, 183 (2016)
- D.-E. Kim, M.-J. Kang, G.-R. Park, N.-K. Kim, B.-J. Lee, Y.-S. Kwon, H.-K. Shin, J. Nanosci. Nanotechnol. **16**, 2900 (2016)
- E. Angioni, M. Chapran, K. Ivaniuk, N. Kostiv, V. Cherpak, P. Stakhira, A. Lazauskas, S. Tamulevičius, D. Volyniuk, N.J. Findlay, T. Tuttle, J.V. Grazulevicius, P.J. Skabara, J. Mater. Chem. C **1**, 1 (2016)
- S. Ye, T. Hu, Z. Zhou, M. Yang, Q. Mei, Y. Liu, L. Liu, B. Zhai, Z. Jia, W. Huang, Org. Electron. **33**, 235 (2016)
- D. Yang, Y. Duan, Y. Yang, N. Hu, X. Wang, F. Sun, Y. Duan, J. Lumin. **166**, 77 (2015)
- H. Wu, L. Ying, W. Yang, Y. Cao, *WOLEDs and Organic Photovoltaics* (Springer, Berlin, 2010)
- M. Ariu, M. Sims, M.D. Rahn, J. Hill, A.M. Fox, D.G. Lidzey, M. Oda, J. Cabanillas-Gonzalez, D.D.C. Bradley, Phys. Rev. B **67**, 195333 (2003)
- A.J. Cadby, P.A. Lane, H. Mellor, S.J. Martin, M. Grell, C. Giebeler, D.D.C. Bradley, M. Wohlgenannt, C. An, Z.V. Vardeny, Phys. Rev. B **62**, 15604 (2000)
- A. Perevedentsev, Y. Sonnefraud, C.R. Belton, S. Sharma, A.E.G. Cass, S.A. Maier, J.-S. Kim, P.N. Stavrinou, D.D.C. Bradley, Nat. Commun. **6**, 5977 (2015)
- D.D.C. Bradley, M. Grell, X. Long, H. Mellor, A.W. Grice, M. Inbasekaran, E.P. Woo, in *Proceedings, Optical Probes of Conjugated Polymers* (1997). <https://doi.org/10.1117/12.295530>
- R. Valaski, M.L. Moreira, L. Micaroni, A.I. Hümmelgen, Braz. J. Phys. **33**, 392 (2003)
- K. Yoshino, S. Nakajima, D.H. Park, K. Yoshino, Jpn. J. Appl. Phys. **27**, L716 (1988)
- A. Fujii, H. Kawahara, M. Yoshida, Y. Ohmori, K. Yoshino, J. Phys. D **28**, 2135 (1995)
- R. Singh, J. Kumar, R.K. Singh, A. Kaur, K.N. Sood, R.C. Rastogi, Polymer **46**, 9126 (2005)
- G. Wang, C. Yuan, Z. Lu, Y. Wei, J. Lumin. **68**, 49 (1996)
- K. Yoshino, Y. Manda, K. Sawada, M. Onoda, R. Sugimoto, Solid State Commun. **69**, 143 (1989)
- B. Xu, S. Holdcroft, Macromolecules **26**, 4467 (1993)
- M.A.T. da Silva, E.F. Thomazini, M. Albertini, W. Renzi, F. Franchello, I.F.L. Dias, J.L. Duarte, L.C. Poças, S.A. Lourenço, Opt. Mater. **62**, 119 (2016)
- K. Kanemoto, M. Shishido, T. Sudo, I. Akai, H. Hashimoto, T. Karasawa, Chem. Phys. Lett. **402**, 549 (2005)
- B. Van Der Zanden, R. Van De Krol, J. Schoonman, A. Goossens, Appl. Phys. Lett. **84**, 2539 (2004)
- P.L. Santos, L.A. Cury, F.B. Dias, A.P. Monkman, J. Lumin. **172**, 118 (2016)
- R. Noriega, J. Rivnay, K. Vandewal, F.P.V. Koch, N. Stingelin, P. Smith, M.F. Toney, A. Salleo, Nat. Mater. **12**, 1038 (2013)
- A. Monkman, C. Rothe, S. King, F. Dias, *Polyfluorenes* (Springer, Berlin, 2008), pp. 187–225
- B. Yao, B. Zhang, J. Ding, Z. Xie, J. Zhang, L. Wang, Org. Electron. Phys. Mater. Appl. **14**, 897 (2013)
- X. Chen, H. Wan, H. Li, F. Cheng, W. Nie, B. Yao, Z. Xie, L. Wang, J. Zhang, Org. Electron. Phys. Mater. Appl. **13**, 475 (2012)
- X. Zhang, Z. Lei, Q. Hu, J. Lin, Y. Chen, L. Xie, W. Lai, W. Huang, Appl. Phys. Express. **7**, 101601 (2014)